C. Wiegmann, Y. Suzuki, J. Geiger, E.R. Solano, Y. Liang, Y. Sun, D. Reiter,
R.C. Wolf and JET EFDA contributors

3D MHD Equilibrium Calculations for Tokamaks with the HINT2 Code

3D MHD Equilibrium Calculations for Tokamaks with the HINT2 Code

C. Wiegmann[1], Y. Suzuki[2], J. Geiger[3], E.R. Solano[4], Y. Liang[1], Y. Sun[1], D. Reiter[1], R.C. Wolf[3] and JET EFDA contributors*

JET-EFDA, Culham Science Centre, OX14 3DB, Abingdon, UK

[1]*Institute for Energy Research - Plasma Physics, Forschungszentrum Jülich GmbH, Assoziation EURATOM-FZJ, Trilateral Euregio Cluster, 52425 Jülich, Germany*
[2]*National Institute for Fusion Science, 322-6 Oroshi-cho, Toki 509-5292, Japan*
[3]*Max-Planck-Institut für Plasmaphysik, Assoziation EURATOM-IPP, 17491 Greifswald, Germany*
[4]*Laboratorio Nacional de Fusión, Asociación EURATOM-CIEMAT, Madrid, Spain*
* See annex of F. Romanelli et al, "Overview of JET Results" ,
(Proc. 22 [nd] IAEA Fusion Energy Conference, Geneva, Switzerland (2008)).

1. INTRODUCTION

The application of Resonant Magnetic Perturbations (RMP) to tokamaks recently gained a lot of attention due to the possibility of ELM suppression or mitigation [1,2]. The iron core tokamak TEXTOR with circular plasma cross-section is specially suited to study the 3D effects of RMPs due to its Dynamic Ergodic Divertor (DED) [3]. The DED consists of 16 helically aligned perturbation coils installed in-vessel at the high-field side and can be operated in several base modes ($m/n = 12/4$, $6/2$ and $3/1$) with either DC or AC current supply. The addition of the RMP to an axisymmetric equilibrium perturbs the force balance

$$\nabla p \quad \mathbf{J} \times (\mathbf{B} + \mathbf{B}_{pert}). \tag{1}$$

To reestablish the force balance, we recalculate the 3D equilibrium including an equilibrium response to the perturbation field. A full penetration of the RMP is assumed and screening of the RMP is not taken into account. The converged 3D equilibria are compared with the simple vacuum superposition assumption.

2. HINT2

To investigate the resulting 3D equilibrium the HINT2 code [4, 5] is applied. This code is an Eulerian initial value solver which relaxes the given initial magnetic field configuration into an equilibrium by solving resistive MHD equations. HINT2 uses a quasi-eulerian helically rotating grid (u^1; u^2; u^3) which in case of tokamak calculations reduces to a cylindrical like coordinate system. The relaxation process is carried out in two steps. In step A, the pressure is adjusted to satisfy a vanishing pressure gradient along the field lines ($\mathbf{B} \cdot \nabla p = 0$) by evaluating the line averaged pressure along a field line

$$p^{i+1} = \bar{p} = \frac{\displaystyle\int_{-L_{in}}^{L_{in}} F \, p^i \, \frac{dl}{B}}{\displaystyle\int_{-L_{in}}^{L_{in}} \frac{dl}{B}} \quad , \qquad F = \begin{cases} 1 & : \text{if } L_C \quad L_{in} \\ 0 & : \text{if } L_C < L_{in} \, . \end{cases} \tag{2}$$

On field lines which leave the computational domain or intersect with a limiting contour the pressure is set to zero. Depending on the value of L_{in} a finite pressure in the stochastic edge region can be sustained. In step B a set of resistive MHD equations with fixed pressure distribution and artificial resistivity are solve

$$\frac{\mathbf{v}}{t} = -f_{CFL} \, (\mathbf{J} = \nabla p + (\mathbf{J} - \mathbf{J_0} \times \mathbf{B}). \tag{3}$$

$$\frac{\mathbf{B}}{t} = \nabla \times \left\{ \mathbf{v} \times \mathbf{B} - \eta \left(\mathbf{J} - \mathbf{J_0} - \mathbf{B} \frac{\langle \mathbf{J} \cdot \mathbf{B} \rangle_{net}}{\langle B^2 \rangle} \right) \right\} \tag{4}$$

1

$$\mathbf{J} = \nabla \times \mathbf{B}, \quad \mathbf{J_0} = (\nabla + \mathbf{B_{vac}}). \tag{5}$$

The factor f_{CFL} is necessary to ensure that the Courant-Friedrich-Levy condition is satisfied in case that field coils are located inside the computational domain. $\mathbf{J}_0$ denotes the vacuum current density due to the poloidal and toroidal coils within the computational domain. An infinitely conducting wall applies as boundary condition of the computational domain. The net toroidal current density $\mathbf{B} \frac{\langle \mathbf{J} \cdot \mathbf{B} \rangle_{net}}{\langle B^2 \rangle}$ is made up by the ohmic and bootstrap current, currents due to heating and current drive schemes. A functional dependence on the normalized toroidal flux is assumed.

3. TEXTOR

We calculated the 3D equilibrium for TEXTOR with the DED in 6/2 mode configuration for different DED currents, namely I_{DED} = 1.5kA/coil, 4.5kA/coil and 7.5kA/coil for an underlying 2D equilibrium with the following parameters: I_P = 1245kA, B_{tor} (@1.75) = 1.3T and a central axis pressure of p_{axis} = 16kPa. Due to the perturbation field symmetry only a half torus calculation was sufficient. The resolution was chosen to be 129×129×184 grid points (u^1; u^2; u^3) corresponding to a spacial resolution of 1.02cm in a poloidal plane and about 1° in toroidal direction. In step A, L_{in} = 400m was used for the pressure relaxation to ensure that the inner islands are traced out completely and the pressure profile is flattened there accordingly.Figure 1a shows the Poincare plot representation of the resulting topology for the case with I_{DED} = 1.5kA/coil for the HINT2 result. While the major structures are conserved in the HINT2 calculation, an additional ergodisation around the X-points of the major islands (e.g. the 3/2 islands) appears as can be clearly seen in figure 1b. Furthermore, secondary structures in the islands appear, a feature already observed experimentally for 2/1 islands in DED 3/1 mode [6]. This effect is caused by the modified Pfirsch Schlüter current density distribution driven by the pressure gradient around the islands. In figures 2a and 2b connection length plots for an enlarged edge area are shown and indicate an increased island size in the HINT2 case. Furthermore, a statistical analysis shows an increase in short (≤1000m) and very long (≈16000m) field lines (see figure 2c) in the HINT2 case. This indicates a sharper transition from the confined core to the vacuum region.

4. JET

A stronger equilibrium response can be expected from an H-mode plasma with strong gradients at the plasma edge. Therefore, we applied HINT2 to an equilibrium case with high edge current density and a steep pressure gradient. First, an axisymmetric equilibrium was recalculated to obtain a higher resolution equilibrium compared to the original EFIT solution. Here an EFIT reconstruction of Pulse No: 58837 was used [7]. In a second step, an n = 2 perturbation field (I_{EFCC} = 32kA/coil) was added. A full torus calculation was conducted as the error field correction coils are not completely symmetric. The resolution was chosen to be 157×201×180 grid points (u^1; u^2; u^3) corresponding to

2

a spacial resolution of $\approx$1.5cm along the major radius, about 2cm in vertical and about 2 in toroidal direction. For step A, a pressure relaxation length of L_C = 200m was chosen. Therewith a pressure build-up in the private flux region of the SOL is prevented and a finite pressure is still maintained at the ergodised plasma boundary.

Figure 3a and 3b show the Poincare plot visualisations of the resulting magnetic field distributions at ϕ = 0. It is remarkable, that no major differences can be observed against our original expectation. High resolution connection length plots for the X-point and divertor region do not show major differences on a first glance. Some structures are shifted on a 0.5cm scale (e.g. left divertor leg). A statistical comparison of the distribution of field lines in specified field line length intervals shows clear differences. In the HINT2 case the number of field lines with connection lengths <1800m is increased while the vacuum modelling shows a larger fraction of field lines at higher values. This is an indication for an increased ergodisation at the X-point and can explain the experimentally observed density pump-out already at perturbation field levels below complete ergodisation (Chirikov parameter above 1). However, further studies with increased grid resolution of the HINT2 calculation will be necessary in order to better resolve the island structures on the low field side.

CONCLUSION

For the TEXTOR case the HINT2 calculations show clear modifications compared to the vacuum superposition. For JET further calculations with higher resolution will be necessary to obtain a clearer picture of the differences between the vacuum superposition and the HINT2 result.

REFERENCES

[1]. Y.Liang et al., Physics Review Letters **98**,265004 (2007)

[2]. T.E. Evans et al., Nature Phys. **2**, 419 (2006)

[3]. K.H. Finken et al., The structure of magnetic field in the TEXTOR-DED, Schriften des Forschungszentrum Jülich, Energy Technology **45**, ISSN 1433-5522 (2005)

[4]. K. Harafuji et al., J. Comp. Phys. **81**, 169-192 (1989)

[5]. Y. Suzuki et al., Nuclear Fusion **46**, L19-L24 (2006)

[6]. Y. Liang et al., Nuclear Fusion **47**, L21-L25 (2007)

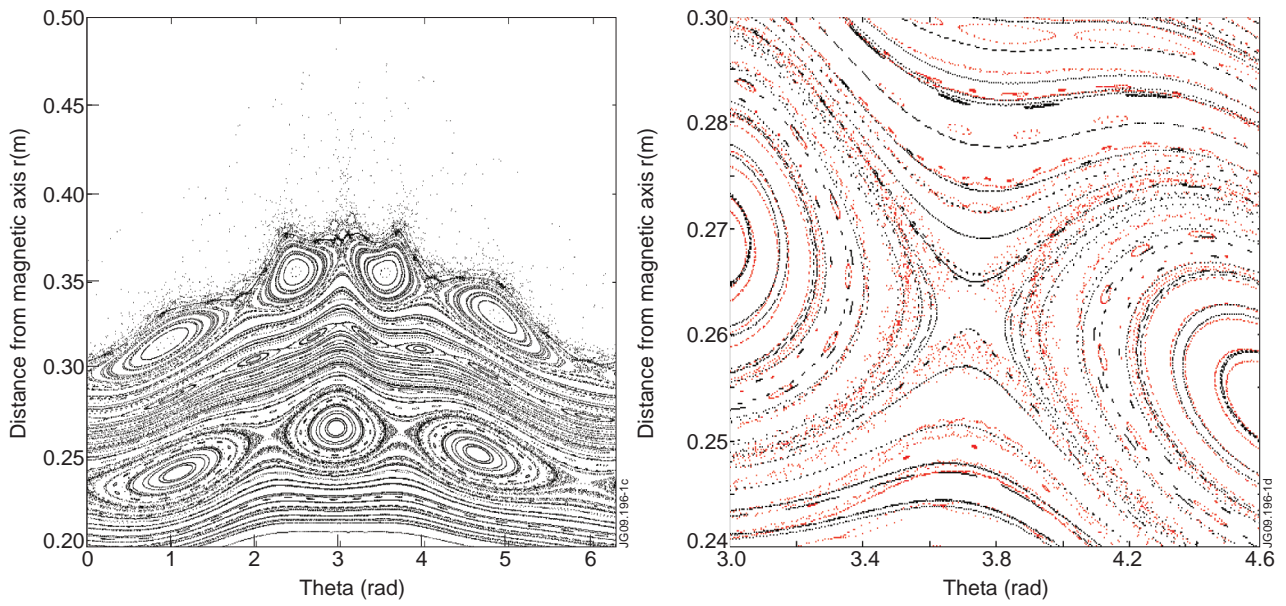[7]. E.R. Solano et al., Nuclear Fusion **48**, 065005 (2008)

Figure 1: Poincare plots at $\phi = 0^o$ for IDED = 7.5kA/coil: (a) HINT2, (b) Vacuum superposition (black dots) superposed with the HINT2 result (red dots) around an X-point region.
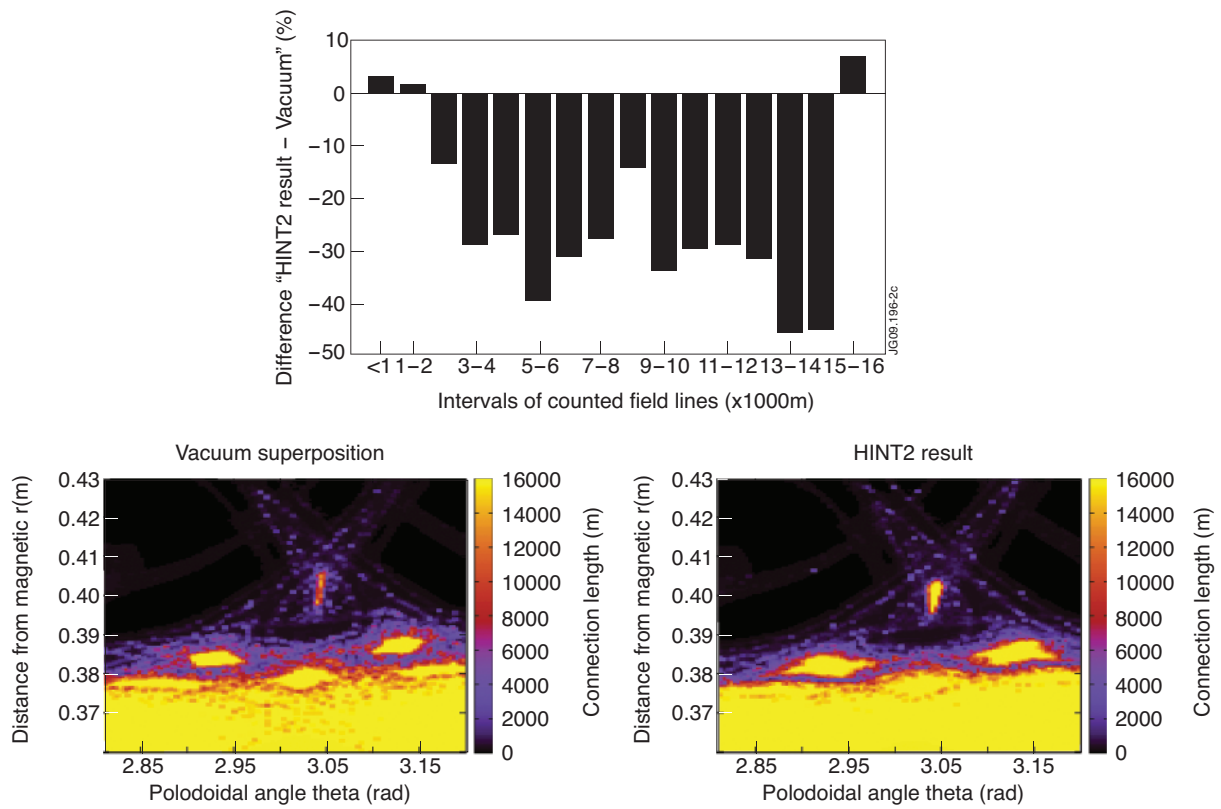

Figure 2: Connection length plots: (a) vacuum, (b) HINT2. (c) Difference of the number of field lines in specified length intervals: HINT2 result minus vacuum superposition in percent.
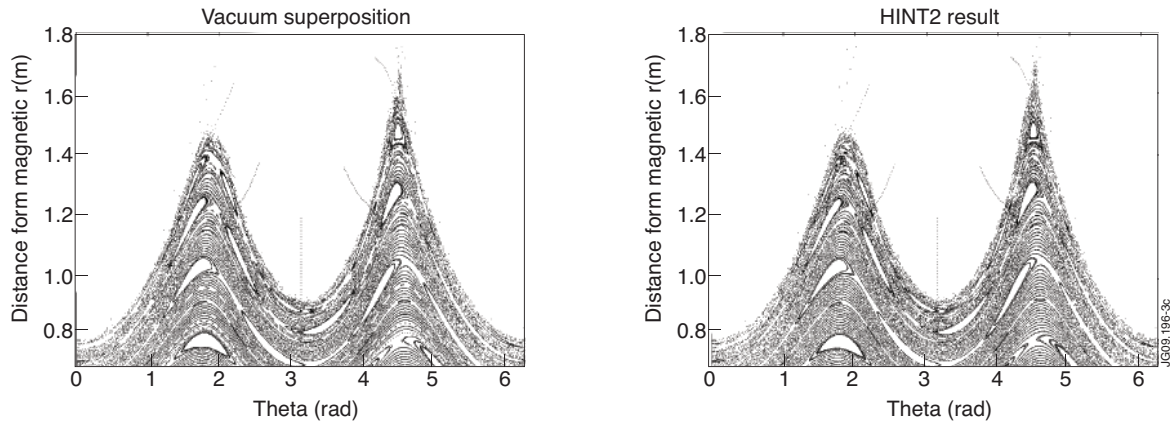
4

Figure 3: Poincare plots at φ = 0: (a) vacuum, (b) HINT2.
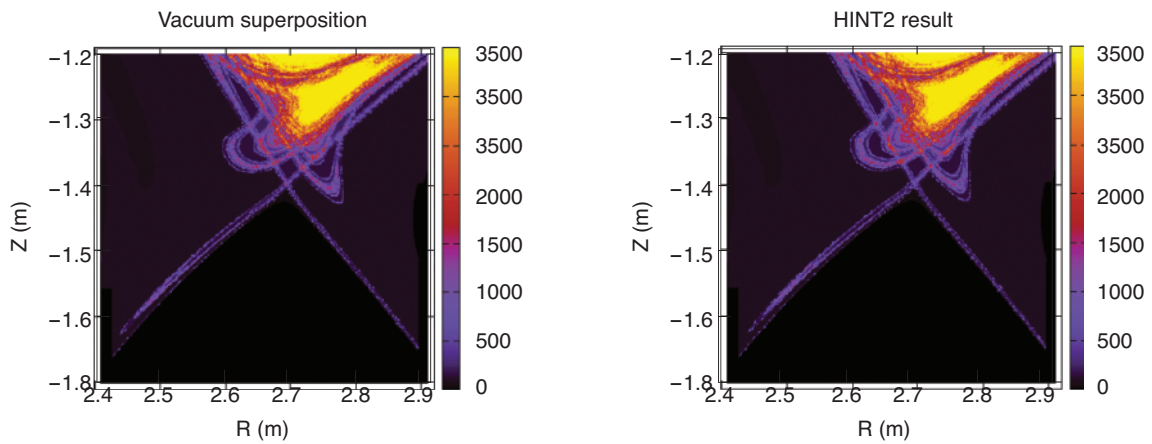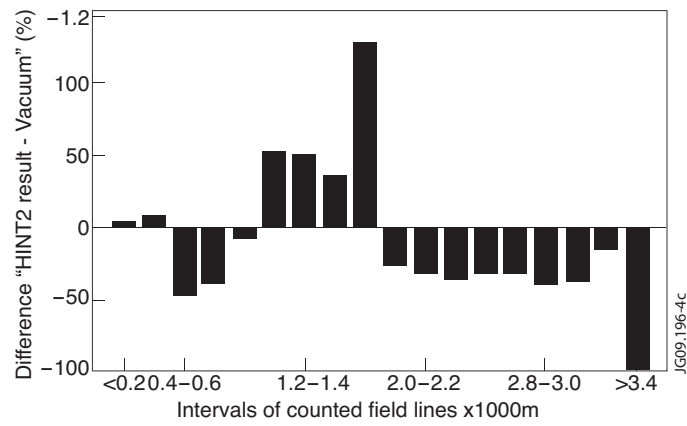

Figure 4: Connection length plots of the X-point region (a) vacuum, (b) HINT2. (c) Procentual difference of the number of field lines in specified length intervals: HINT2 result minus vacuum superposition.